$^2H(p,\gamma)^3He$ reaction using polarized and unpolarized protons

D. M. Skopik
Saskatchewan Accelerator Laboratory, University of Saskatchewan, Saskatoon, Canada S7N OWO and Triangle Universities Nuclear Laboratory, Duke Station, Durham, North Carolina 27706

H. R. Weller
Department of Physics, University of Florida, Gainesville, Florida 32611 and Triangle Universities Nuclear Laboratory, Duke Station, Durham, North Carolina 27706

N. R. Roberson and S. A. Wender
Department of Physics, Duke University, Durham, North Carolina 27706 and Triangle Universities Nuclear Laboratory, Duke Station, Durham, North Carolina 27706

(Received 31 July 1978)

The 90° yield curve for the $^2H(p,\gamma)^3He$ reaction has been studied over the excitation region in ^3He of approximately 7 to 15 MeV. Both polarized and unpolarized proton beams were used to measure the angular distributions of cross section and analyzing power at $E_x = 8.83$, 9.83, and 10.83 MeV. If only the four non-spin-flip $E1$ and $E2$ T-matrix elements are considered, their amplitudes and relative phases can be extracted. The $E2$ cross section obtained from this analysis is found to be $(12 \pm 5)\%$ of the total cross section. The detailed balanced differential ($\theta_{lab} = 90°$) and total cross sections at $E_x = 10.83$ MeV are found to be (117 ± 11) μb/sr and (1.07 ± 0.11) mb, respectively; the quoted errors represent the total uncertainties in the cross sections obtained in this experiment. The results are also compared with recent $E1$ and $E2$ calculations.

[NUCLEAR REACTIONS $^2H(p,\gamma)^3He$; measured $\sigma(90°)$, $E_x \cong 7$–15 MeV; $\sigma(\theta)$, $A(\theta)$, and σ(tot), $E_x = 8.83$, 9.83, and 10.83 MeV; deduced $E1$ and $E2$ T-matrix amplitudes and phases.]

I. INTRODUCTION

Experimental studies of the reaction $^3He(\gamma,d)p$ (and its inverse p-d capture) have yielded diverse results. The magnitude of the differential cross section at 90°, near the peak of the giant resonance ($E_\gamma \simeq 12$ MeV), ranges from ≈90 μb/sr to 120 μb/sr with no clear separation of the measurements into low and high values. This is illustrated in Fig. 1 which summarizes all of the data published as photodisintegration results.[1–10] Note that these data include two electrodisintegration measurements[3,9] in which the final state electron was not detected, and an $E1$ virtual photon analysis was applied to the data to obtain equivalent photon cross sections. That these experiments would tend to lie somewhat higher than the real photon results is demonstrated in Ref. 11, where an electrodisintegration measurement was compared to the photodisintegration results through a model. While this comparison demonstrated the need for including monopole transitions in the virtual photon analysis (the implication is that if the monopole spectrum were included the converted electrodisintegration results could be somewhat lower depending upon the kinematic factors, especially the incident electron energy used in the experiment), the magnitude of this correction in the converted electrodisintegration experiments is only a few percent.

The theoretical effort for the mass-3 system has seen an improvement inasmuch as exact, within the model, Faddeev type calculations are now available. Gibson and Lehman[12] considered only $E1$ transitions for the two-body breakup of ^3He and found a peak 90° cross section of ≈95 μb/sr, while an earlier calculation by Barbour and Phillips[13] gave a peak value of ~120 μb/sr. The difference in these results is ascribed to the different ground state wave functions that were used (note that Barbour and Phillips, unlike Gibson and Lehman, included the S' state as well.) The effects of short range repulsion and the tensor force in the ground state were included in a calculation by Hendry and Phillips,[14] and were shown to affect the p-d breakup channel by approximately 10%. In addition Barbour and Hendry[15] have examined the effects of $E2$ transitions and find that final state interactions play a very important role, but that the $E2$ cross section contributes very little (1–2%) to the total cross section.

In view of the experimental discrepancies in the normalization of the two-body breakup channel in ^3He and its importance in drawing a conclusion about the validity of a particular model, we have made a precise p-d capture measurement of the

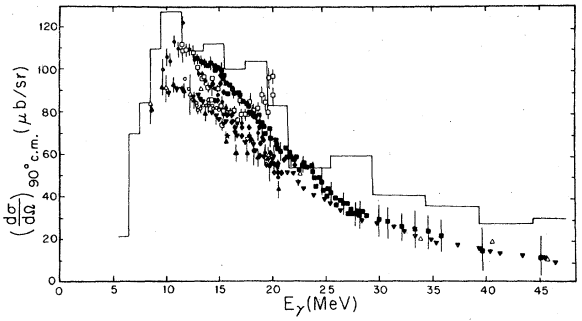

FIG. 1. Summary of data published as photodisintegration results; ⎍ —Ref. 1, □ —Ref. 2, △—Ref. 6, ■—Ref. 3, ▲—Ref. 5, ○—Ref. 8, ●—Ref. 9, *—Ref. 10, ♦ —Ref. 7, ▼ —Ref. 4.

absolute cross section from $E_p = 3.0$ to 14.8 MeV. In addition, we have measured the angular distributions of cross section and analyzing power at $E_p = 5.0$, 6.5, and 8.0 MeV.

The angular distributions of cross section and cross section times analyzing power can be expressed in terms of reduced transition (T) matrix elements. The amplitudes of these complex matrix elements can be labeled in the L-S coupling scheme by the incoming quantum numbers L, S, and J, and the outgoing multipolarity. For the case of p-d capture, the incident spin of $\frac{1}{2}$ coupled to the target spin of 1 results in a large number of interference terms among the contributing T-matrix elements even when only $E1$ and $E2$ transitions are considered. It is such interference terms which can give rise to finite analyzing powers. Since interference terms which can, in principle, be large remain even after the restriction to non-spin-flip $E1$ and $E2$ transitions ($S = \frac{1}{2}$) is made, it might be expected that considerable analyzing power could result in the present case. It is interesting to note that appreciable polarization has been observed[16,17] for the photodisintegration of the deuteron and in the ^{3}H$(p,\gamma)^4$He reaction. In the former, the polarization of the photoneutrons is attributed to the presence of $M1$ transitions, while in the latter it appears to arise primarily from the interference of $E1$ amplitudes having different channel spins.

The conclusion that considerable analyzing power could result in the present case can be violated in three ways: (1) One of the T-matrix amplitudes in each interference term could be very small; (2) the phase differences could be very small; or (3) the various interference terms which contribute to the analyzing power could have magnitudes and signs which sum to (essentially) zero. It will be seen that the small analyzing powers observed in the present work are apparently the result of (2) above for $E1$-$E1$ interference terms and (3) above for $E1$-$E2$ type terms.

As a result of these analyzing power measurements the problem of extracting the $E2$ cross section near the peak of the giant resonance in ^{3}He requires fewer assumptions than has been possible with previous unpolarized measurements. It will be seen that an analysis which includes what are expected to be the major $E1$ and $E2$ amplitudes (non-spin-flip), and their relative phases, indicates that the $E2$ cross section near $E_\gamma \simeq 11$ MeV is significantly larger than the value predicted by theory.

II. EXPERIMENT

The capture γ-ray facility at the Triangle Universities Nuclear Laboratory was used to measure energy spectra and angular distributions of the γ rays for the reaction ^{2}H$(p,\gamma)^3$He. Polarization data were taken using a Lamb-shift polarized ion source which produced a beam having a polarization of 0.80 ± 0.02. Since both of these systems have been described in previous papers[18,19] only the essential features and calibrating techniques will be presented here.

γ rays were detected in a 25.4×25.4 cm NaI crystal having a plastic anticoincidence shield. The front face of the NaI crystal was collimated such that the back face of the detector was fully illuminated by the γ rays emitted from the target. A typical γ-ray spectrum from a CD_2 target is shown in Fig. 2.

The CD_2 targets (92% enrichment) were fabricated by dissolving CD_2 powder in xylene and then

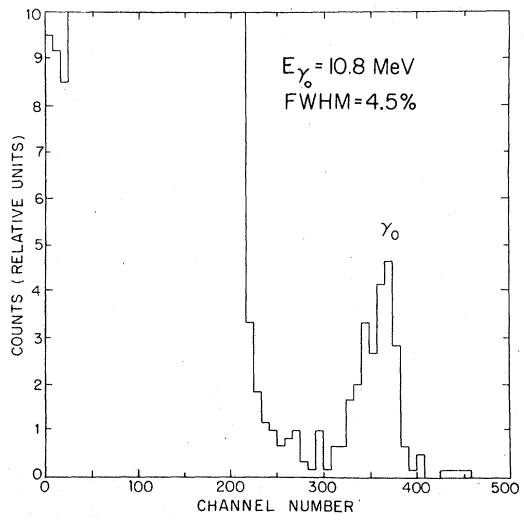

FIG. 2. γ-ray spectra at $E_p = 8.0$ MeV and $\theta = 90°$, showing the clear separation between γ_0 and background obtained in this experiment.

allowing the xylene to boil off in a glycerine bath.[20] This technique produced thin (~1 mg/cm^2), uniform targets which were used in this experiment for proton energies $E_p \lesssim 10$ MeV. At higher proton energies, capture γ rays from the $^{12}C(p,\gamma)$ reaction precluded the use of CD_2 targets, and a 1 atmosphere deuterium gas cell (~0.2 mg/cm^2) was used to measure the cross section up to $E_p = 15$ MeV.

The gas cell was a 3.5 cm high right circular cylinder whose radius was 2.54 cm. The cell wall consisted of 6.5 μm Havar and was shielded from the detector by approximately 20 cm of lead. These gas cell data were normalized to the data taken with the CD_2 target at $E_p = 10$ MeV. All of the angular distributions were taken with the solid target in order to avoid any uncertainties in making angular acceptance corrections to the data.

It was necessary to use a pulsed and bunched beam with a time-of-flight criterion for the most forward angle (30°) at the lowest proton energy of this experiment. This technique eliminated a neutron induced background which overlapped the γ-ray peak. The 30° data, obtained by pulsing the beam at $E_p = 5.0$ MeV, was normalized to the d.c. polarized beam results at several overlapping angles. No attempt was made to obtain an analyzing power for this angle. As a further check, to make certain the γ-ray peak was free from any contaminant counts, runs were taken at several angles forward of 90° with a CH_2 target having the same thickness as the CD_2 target. No counts were observed in the region corresponding to γ_0 in Fig. 2.

Collimated solid state detectors were placed at symmetric scattering angles of 25° on each side of the incident proton beam. This allowed us to measure the polarization of the incident proton beam since the polarization of the $^2H(p,p)$ reaction is well known at these energies and scattering angles.[21] The polarization measured in this way agreed with the polarization measured by the quench-ratio-technique to within 2%. A typical elastic spectrum is shown in Fig. 3. The deuteron recoils and the elastically scattered protons from ^2H, H, and ^{12}C are clearly resolved.

Elastic scattering data also permitted in principle a determination of the target thickness to the accuracy of the known elastic cross sections (~1%) and allowed us to monitor the target conditions during the course of the experiment. Since the target thickness is usually one of the least well known quantities in an absolute experiment, a number of cross checks were made. These included (a) measuring the elastic cross section $^2H(p,p)$ and observing both the protons and the recoiling deuterons at the scattering angles of 25°

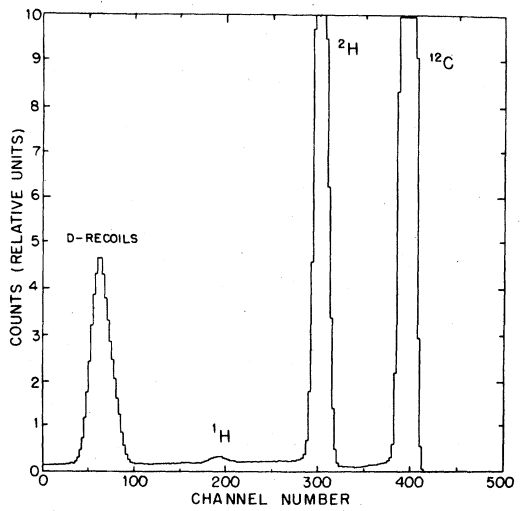

FIG. 3. Elastically scattered protons from ^2H, ^1H, and ^{12}C. Also measured are the deuteron recoils. These data were taken simultaneously with the γ-ray data in order to constantly monitor the target thickness.

and 30°, and (b) measuring the same cross sections with different collimator sizes in front of the solid state detectors. All of the measurements gave results for the target thickness that varied by no more than 3%. The resulting value for the target thickness was (1.10 ± 0.02) mg/cm^2.

The other important factor in performing an absolute cross section measurement, the efficiency of the NaI spectrometer, was determined using the technique proposed by Marrs *et al.*[22] In this procedure the thick target yield from the reaction $^{12}C(p,\gamma_0)^{13}N$ was used at $E_\gamma = 15.07$ MeV (6.833 ± 0.22 × 10^{-9} photons/incident proton) to determine the efficiency of the spectrometer to be 0.17 ± 0.012. The same electronic and solid angle configuration was then used in measuring the $^2H(p,\gamma)^3He$ cross section. In order to verify this value for the efficiency, the contributing factors were considered. The fraction of the total response which appeared in the peak region was obtained from a spectrum obtained by Hayward *et al.*[23] using monochromatic 15.1 MeV γ rays and a 25.4 × 25.4 cm NaI crystal. This number was then corrected for the rejection rate due to the plastic shield in our experiment, a number which we obtained by examining the rejected and unrejected spectra. Finally the attenuation effects of the shielding material placed in front of our detector were measured and taken into account. The result of this analysis gave an overall efficiency which agreed with the quoted result within the error. The total uncertainty in the absolute cross section of the present experiment obtained with this

spectrometer system is ±10%.

The analysis of the γ-ray spectra was performed two ways. First, for all of the angular distributions the spectrum shown in Fig. 2 was fitted with a standard line shape determined from the $^3H(p,\gamma)^4He$ reaction.[24] A constant line shape width was used for all angles. Second, for the excitation curve measurements, the data were summed for a fixed energy window since the separation of the peak from background γ rays presented no problems. The corresponding efficiency was used to form an absolute cross section.

III. DATA ANALYSIS

A. Angular distribution measurements

After center-of-mass corrections were made, angular distributions were least-squares fitted to the expressions

$$\sigma(\theta) = A_0\left[1 + \sum_{l=1}^{4} a_l Q_l P_l(\cos\theta)\right] \quad (1)$$

and

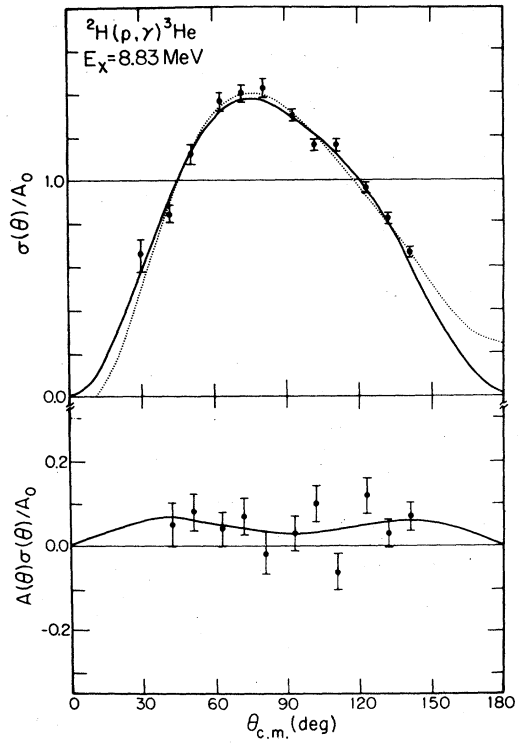

FIG. 4. Cross section and asymmetry data at E_x = 8.83 MeV. The dotted line represents the curve generated by fitting the data to a Legendre polynomial expansion. The solid line corresponds to the fit constrained (see text) at $\theta = 0°$ and 180°. The asymmetry data are unaffected by this constraint.

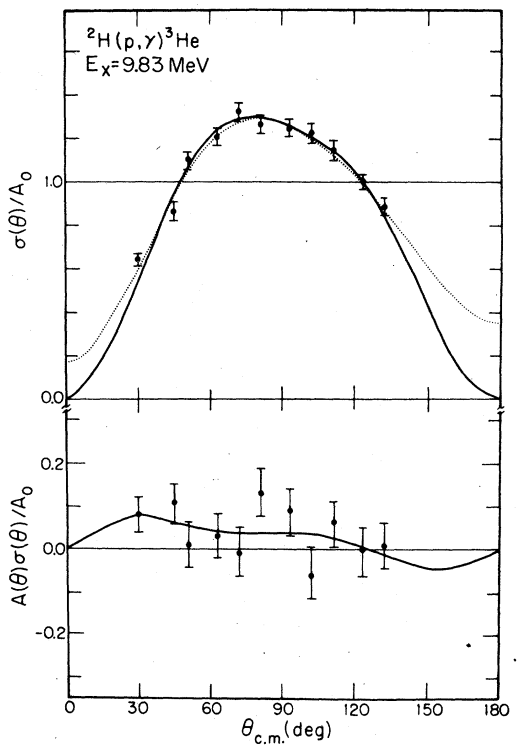

FIG. 5. Cross section and asymmetry data at E_x = 9.83 MeV. Curves are the same as Fig. 4.

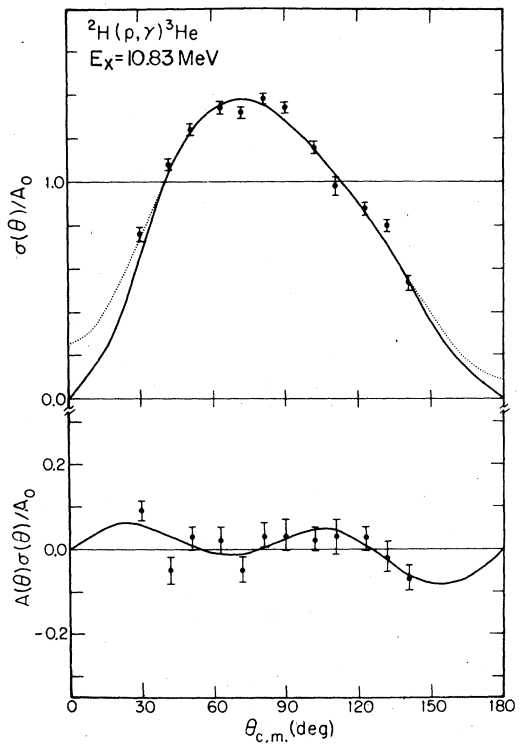

FIG. 6. Cross section and asymmetry data at E_x = 10.83 MeV. Curves are the same as Fig. 4.

TABLE I. Angular distribution coefficients at the three energies of this experiment.[a]

E_x (MeV)	χ^2	A_0 (μb)[c]	a_1	a_2	a_3	a_4	χ^2	b_1	b_2	b_3	b_4
8.83	1.42	76.8±1.5	0.08±0.03	−0.79±0.07	−0.27±0.06	−0.16±0.08	1.86	0.05±0.02	0 ±0.01[d]	0.02±0.01	0 ±0.01
8.83[b]	1.93	82.5±0.8	0.14±0.02	−0.80±0.03	−0.15±0.02	−0.20±0.03			(as above)[d]		
9.83	0.49	85.2±2.5	0.04±0.07	−0.63±0.12	−0.13±0.09	−0.11±0.09	1.11	0.04±0.02	0.02±0.02	0 ±0.02	0.01±0.01
9.83[b]	0.71	86.4±1.1	0.08±0.02	−0.77±0.02	−0.09±0.02	−0.24±0.03			(as above)[d]		
10.83	2.76	86.7±1.4	0.25±0.03	−0.69±0.06	−0.18±0.05	−0.15±0.07	1.5	0.01±0.01	0.01±0.01	0 ±0.01	0.02±0.01
10.83[b]	4.26	86.1±0.6	0.24±0.02	−0.75±0.03	−0.24±0.02	−0.25±0.03			(as above)[d]		

[a] The errors reported here were obtained by multiplying the standard deviations by the value of χ.
[b] Results obtained when data sets were constrained at 0° and 180° (see text).
[c] $\sigma_T(\gamma,p) = 4\pi A_0$.
[d] Results were unchanged by the use of the constraint.

$$A(\theta)\sigma(\theta)/A_0 = \sum_l b_l Q_l P_l^1(\cos\theta)\,, \tag{2}$$

where the Q_l's arise from geometrical effects due to the finite angular acceptance of the crystal. $A(\theta)$, the analyzing power, is defined as

$$A(\theta) = \left(\frac{N_+ - N_-}{N_+ + N_-}\right)\frac{1}{P}\,, \tag{3}$$

where N_+ and N_- are the number of counts obtained for incident protons with spin up and spin down respectively. P is the beam polarization. The data, along with the curves generated by applying expansions (1) and (2), are shown in Figs. 4–6. The a_l and b_l coefficients are presented in Table I. Since it is expected that the cross section is nearly zero at 0° and 180°, a second fit was performed in which the cross section was constrained to be essentially zero at these angles but with errors taken to be indicative of the errors in the present experiment. This procedure is supported by the precise, detailed angular distributions obtained by Belt *et al.*[29] at $E_x = 12.1$ MeV. The fits obtained using this procedure are also shown in Figs. 4–6, and the coefficients are included in Table I. Since the fits to the product of cross section and analyzing power were not affected by the constraints, no results are reported for this case.

Although a large number of T-matrix elements are possible in this reaction channel, we have restricted the number included in the analysis for the following reasons. First, as pointed out by Schiff,[25] for a pure symmetric S ground state, $M1$ transitions are expected to be quite small for this reaction due to orthogonality of the initial and final states. An isotropic contribution to the angular distribution from spin-flip $M1$ transitions can thus arise only from the mixed symmetry S' state which would be most important near threshold. However, thermal neutron capture studies[26] have shown that spin-flip $M1$ transitions are very small near threshold and thus may be neglected for higher excitation energies in the mass 3 system. Also, the results obtained by Belt *et al.*[29] indicate that the ratio of the isotropic to nonisotropic components (their a/b) is 0.013± 0.01, a result which can be accounted for by including 6% D state and 2% S' state in the ground state wave function of ^{3}He.[30] This admixture of D state may also give rise to an isotropic component in the angular distribution. These transitions ($^4D_{1/2} \rightarrow F, P, S$ final states), however, have been shown to be small for $E_\gamma \lesssim 15$ MeV.[3] These results indicate that neglecting spin-flip $E1$, $E2$, and $M1$ radiation is thus a reasonable first approximation in analyzing these data. Higher multipoles, specifically $M2$ and $E3$, have been neglected in this

analysis. They will be discussed later.

In channel spin representation, considering only non-spin-flip ($S=\frac{1}{2}$) $E1$ and $E2$ terms, we have the following complex reduced T-matrix elements denoted by R_{LJ} for the proton partial waves:

$$R_{1,1/2}e^{i\psi_0},\quad R_{1,3/2}e^{i\psi_1},\quad R_{2,3/2}e^{i\psi_2},\text{ and } R_{2,5/2}e^{i\psi_3},$$

where the first two are for $E1$ and the second two are for $E2$ radiation. Considering only these matrix elements one can deduce[27]

$$\begin{aligned}
1.0 &= 2R^2_{1,1/2}+4R^2_{1,3/2}+4R^2_{2,3/2}+6R^2_{2,5/2}\quad\text{(normalization)},\\
a_1 &= 6.92\,R_{2,3/2}R_{1,1/2}\cos(\psi_2-\psi_0)+1.38R_{2,3/2}R_{1,3/2}\cos(\psi_2-\psi_1)+12.48R_{2,5/2}R_{1,3/2}\cos(\psi_3-\psi_1),\\
a_2 &= -2R^2_{1,3/2}+2R^2_{2,3/2}+3.42R^2_{2,5/2}-4R_{1,3/2}R_{1,1/2}\cos(\psi_1-\psi_0)+1.72R_{2,5/2}R_{2,3/2}\cos(\psi_3-\psi_2),\\
a_3 &= -6.92R_{2,5/2}R_{1,1/2}\cos(\psi_3-\psi_0)-8.32R_{2,3/2}R_{1,3/2}\cos(\psi_2-\psi_1)-5.54R_{2,5/2}R_{1,3/2}\cos(\psi_3-\psi_1),\\
a_4 &= -3.42R^2_{2,5/2}-13.72R_{2,5/2}R_{2,3/2}\cos(\psi_3-\psi_2)
\end{aligned}\qquad\text{Eq. set (4)}$$

and[28]

$$\begin{aligned}
b_1 &= -1.16R_{2,3/2}R_{1,1/2}\sin(\psi_2-\psi_0)-0.92R_{2,3/2}R_{1,3/2}\sin(\psi_2-\psi_1)+2.08R_{2,5/2}R_{1,3/2}\sin(\psi_3-\psi_1),\\
b_2 &= -0.66R_{1,3/2}R_{1,1/2}\sin(\psi_1-\psi_0)+0.47R_{2,5/2}R_{2,3/2}\sin(\psi_3-\psi_2),\\
b_3 &= -0.77R_{2,5/2}R_{1,1/2}\sin(\psi_3-\psi_0)+0.92R_{2,3/2}R_{1,3/2}\sin(\psi_2-\psi_1)-0.15R_{2,5/2}R_{1,3/2}\sin(\psi_3-\psi_1),\\
b_4 &= -1.14R_{2,5/2}R_{2,3/2}\sin(\psi_3-\psi_2)
\end{aligned}\qquad\text{Eq. set (5)}$$

Rather than using the previously determined a_l and b_l coefficients and solving Eqs. (4) and (5) to obtain the amplitudes and phases, we fit the cross section and the analyzing power data directly in terms of the amplitudes and the phases. This procedure ensures that the full error matrix is correctly propagated through the analysis. When only the four non-spin-flip $E1$ and $E2$ matrix elements are included in the analysis and the fits are constrained such that $\sigma(\theta)$ is essentially zero at $\theta=0°$ and 180° (see the previous discussion), we obtain two solutions for the matrix element amplitudes and phases which are given in Table II. The χ^2 values per degree of freedom given in this table result from including only the statistical errors in the analysis. A comparison of these χ^2 values with the total χ^2 obtained when fitting the constrained data to the polynomial expansions (see Table I) indicates that the quality of the fits is comparable. As seen in Table II this analysis indicates that the two $E1$ matrix elements ($R_{1,1/2}$ and $R_{1,3/2}$) are equal to within an error of about 5%, and that the two $E2$ matrix elements ($R_{2,3/2}$ and $R_{2,5/2}$) are equal to within an error of about 15%. Furthermore, while the relative phase between the two $E1$ or two $E2$ matrix elements is small, the $E1$-$E2$ phase is approximately $\pm 70°$–$85°$.

From these results we may deduce the total $E2$ cross section at the three excitation energies which we have measured. The errors associated with these results include, in addition to the statistical error, an error which reflects the varia-

TABLE II. Amplitudes (% of σ_{tot}) and phases found from least-squares fitting directly to the data using Eqs. (1) and (2) and Eq. sets (4) and (5). The fits were constrained such that $\sigma(0°)$ and $\sigma(180°)$ are zero.[a]

	$(2j+1)R^2_{LJ}$(%)				Phase angle (deg) relative to ψ_0			
E_x (MeV)	$2R^2_{1,1/2}$	$4R^2_{1,3/2}$	$4R^2_{2,3/2}$	$6R^2_{2,5/2}$	ψ_1	ψ_2	ψ_3	χ^2
8.83	29±2	63±3	3.1±1	5.3±1	−2±3	75±5	82±3	4.2
	30±1	61±2	4.1±1	10.0±1	−3±1	−83±3	−83±3	4.3
9.83	28±2	60±3	4.3±1	7.6±1	−3±2	81±5	84±3	1.6
	30±1	58±1	5.5±1	6.9±1	−3±0.5	−87±2	−86±3	1.6
10.83	27±2	61±3	4.8±2	7.1±2	−1±1	70±10	77±3	7.3
	31±1	57±2	5.2±1	6.8±1	−3±1	−81±2	−74±1	7.4

[a] The errors reported here were obtained by multiplying the standard deviations by the value of χ.

TABLE III. Comparison of $E2$ strength near the maximum γ-ray energy measured in this experiment.

Reference	E_x (MeV)	$E2$ cross sections (% of total)
Ref. 1 [a]	12–16	15 ±10
Ref. 2 [a]	12.1	3.2±1.0
Ref. 2 [a]	15.3	5.0±0.8
Ref. 3 [a]	15.0	7.9±2.8
Present work	10.8	12 ±5

[a] The $E2$ strength was estimated from these experiments using Eqs. (6) and (7).

tion in $E2$ strength which is obtained when the constraints at 0° and 180° are not included in the analysis. In Table III, we give these results along with the values that have been estimated from other experiments that are near the excitation energies that we have measured. The estimates from the other experiments were made by considering the multipole expansion

$$\sigma(\theta) = a + b\sin^2\theta + c\sin^2\theta\cos\theta + d\sin^2\theta\cos^2\theta \quad (6)$$

and noting that if d arises solely from $E2$ transitions then

$$\sigma(E2) = \frac{1}{5}\frac{d}{b}\sigma(E1) \; . \quad (7)$$

So we see that if we attribute all of the cross section to non-spin-flip $E1$ and $E2$ terms, our results agree with previous work except for the case of Ref. 2. It should be emphasized that we have *assumed* that only non-spin-flip $E1$ and $E2$ radiation is involved in our extraction of the $E2$ strengths.

In Fig. 7 we show the calculation by Barbour and Hendry[15] for the total $E2$ cross section. Their peak cross section of 20 μb is considerably less than our 12% result which implies an $E2$ cross section near 11 MeV of $\approx(120\pm25)$ μb. The interesting thing to note about their calculation is the fact that inclusion of final state interactions greatly decreases the cross section from the plane wave value in contrast to what is found for the $E1$ case. Using the same parameters for the Irving-Gunn ground state wave function that gave good agreement with the electrodisintegration results of Ref. 12, the plane wave total $E2$ and $M2$ cross sections have been calculated.[31] The result for $\sigma(E2)$ is the same as the plane wave calculations of Barbour and Phillips. The $M2$ cross section was calculated since the analysis of a recent inelastic electron scattering experiment from ^{3}He (Ref. 32) found that the $M2$ strength dominated the $E2$ strength in this excitation region when $q^2 > \omega^2$. Hence to ascertain that we were justified in neglecting $M2$ strength in our analysis the cross section at the photon point was calculated. From this $M2$ total cross section calculation (given by the dashed line in Fig. 7) we see that the $M2$ contribution can be neglected in this experiment since it is expected to account for less than 1% of the total cross section. We have also calculated, in the same model, $\sigma(E3)$, since $E1$-$E3$ interference would result in a contribution to a_4 in Eq. (1). In this energy region (~10 MeV) the ratio $\sigma(E3)/\sigma(E1) \sim 10^{-6}$, indicating in our model that the contribution to a_4 from $E1$-$E3$ interference is small. However, we point out that another plane wave as well as a Faddeev type calculation have given the result[33] that the ratio β^2/γ [where $\beta = c/b$ and $\gamma = d/b$ referring to Eq. (6)] decreases from 4 to 2.6 when $E1$-$E3$ interference is taken into account. Thus it would appear that further calculational effort is required in order to account for the data.

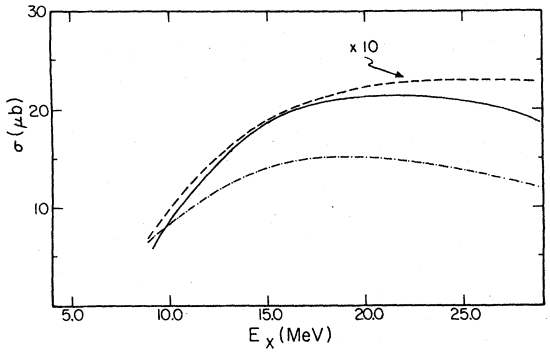

FIG. 7. Calculated $E2$ and $M2$ total cross sections. The (– · –) $E2$ curve is from Ref. 15 with final state interactions, (——) is the $E2$ plane wave calculation of Ref. 15 (Ref. 31 gave identical results for the plane wave $E2$ calculation), (— — —) is $\sigma(M2)\times10$ from Ref. 31.

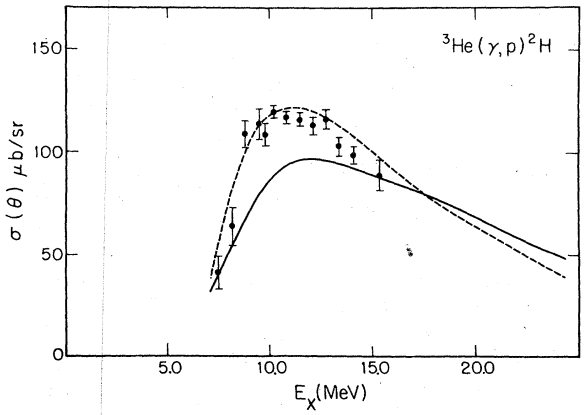

FIG. 8. Differential cross section for the reaction $^3He(\gamma,d)^1H$ at $\theta = 90°$. Curve (— — —) is from Ref. 13, curve (——) is from Ref. 12. These data should be compared with those given in Fig. 1.

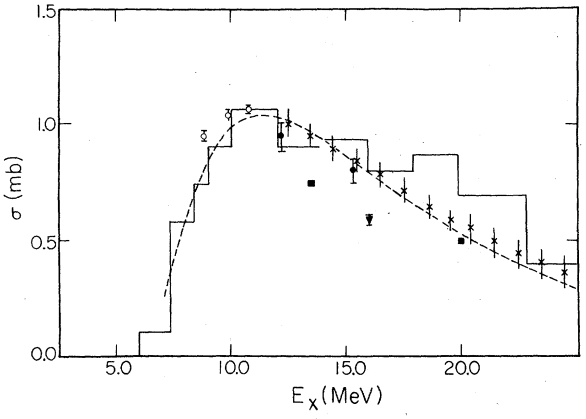

FIG. 9. Total cross section for the reaction ^{3}He(γ, d). Open circles are the present results found from $\sigma(\text{tot}) = 4\pi A_0$, ⊓⊔ —Ref. 1, ●—Ref. 2, ✕—Ref. 3, ■—Ref. 4, and ▼—Ref. 10. Note that only total cross sections are shown. The dashed line is from Barbour and Phillips (Ref. 13).

B. Measurement of $\sigma(\theta = 90°)$ and σ(tot)

To resolve the large discrepancies in the two-body 90° differential cross section, we have also measured the energy distribution over an excitation range in ^{3}He of $E_x = 7.5$ to 15.4 MeV. As noted earlier the energy distribution was measured to $E_x \simeq 12$ MeV with the CD_2 target, while for the higher energies a deuterium gas cell was used and normalized to the solid target results at several overlapping energies. Since the spectrometer efficiency was determined at 15.1 MeV, the efficiencies at other energies have been obtained by correcting for the experimentally determined energy dependence of (1) the crystal response function,[23] (2) the attenuation of the γ rays[34] by the shielding in front of the crystal, and (3) the rejection rate due to the anticoincidence shield. For the lowest energy the efficiency was taken as 14.5% (a 15% correction relative to the calibration point). The energy loss of the primary proton beam in the target was also taken into account.

The results of these measurements are shown in Fig. 8. The two most recent Faddeev calculations are also given. The calculations differ essentially only in the form of the ground state wave function that was used. Our data agree with the earlier cloud chamber measurements (see Fig. 1) of Fetisov *et al.* (Note that a recent calculation by Craver *et al.*[35] which does not include final state interactions reported a peak cross section of ≈70 μb/sr with an anomalous peak at 15 MeV.) Our measurements indicate a total cross section of (1.07 ± 0.01) mb at E_x = 10.83 MeV, where the error is the statistical error only. The overall error, due to the uncertainty in the absolute cross section normalization, is ±10%. Including this error gives a total cross section at $E_x = 10.83$ MeV of (1.07± 0.11) mb.

The total cross sections at the three energies that angular distributions were measured [$\sigma(\text{tot}) = 4\pi A_0$] are given in Fig. 9 by the open circles. We also show in this figure the more recent experiments that were specifically undertaken to resolve the question of normalization. Total cross sections that were obtained from the 90° cross section have not been included in this figure. An earlier capture measurement[36] gave lower results for the total cross section ($\sigma_T \sim 0.70$ mb), but the uncertainties in this experiment were large (±15% statistical errors alone). These data are not shown in Fig. 9. The dashed line again represents the results of the pure $E1$ calculation of Barbour and Phillips[13] (Ref. 12 only calculated the 90° cross section).

IV. CONCLUSION

Our detailed balanced p-d capture results support the higher normalization of this channel which is exemplified by the cloud chamber measurement of Fetisov *et al.*[1] By neglecting $M1$ transitions, $E1$ and $E2$ spin-flip transitions, and all other multipoles, we find that $\sigma(E2)$ is approximately 120 ± 50 μb near the peak of the total cross section in ^{3}He. This value of $\sigma(E2)$ is considerably larger than that predicted by theory, and could essentially already exhaust the total $E2$ energy weighted sum rule of Nathan and Nilsson[37] when integrated over the measured region. Perhaps the neglect of many small terms arising from other transitions is essential here. The phases of the two $E2$ amplitudes relative to the $E1$ amplitudes are found to be about ±80° indicating that a plane wave approximation, as expected, is very poor in this energy region. The analysis indicates that the transition matrix elements for a given L value are equal to within experimental uncertainty, indicating that the matrix elements are independent of J to within the accuracy of this experiment. Hence to a good approximation, one can regard the reaction as proceeding primarily via one $E1$ amplitude and one $E2$ amplitude characterized by $L = 1$ and $L = 2$, both having $S = \frac{1}{2}$. This description would imply zero analyzing power, in good agreement with experiment.

This work was partially supported by the U. S. Department of Energy. We want to thank Drs. R. A. Blue, C. P. Cameron, D. R. Tilley, J. D. Turner, and P. Von Behren for their assistance.

[1]V. N. Fetisov, A. N. Gorbunov, and A. T. Varfolomeev, Nucl. Phys. 71, 305 (1965).
[2]A. van der Woude, M. L. Halbert, C. R. Bingham, and B. D. Belt, Phys. Rev. Lett. 26, 909 (1971).
[3]S. K. Kundu, Y. M. Shin, and G. D. Wait, Nucl. Phys. A171, 384 (1971).
[4]G. Ticcioni, S. N. Gardiner, J. L. Matthews, and R. O. Owens, Phys. Lett. 46B, 369 (1973).
[5]B. L. Berman, L. J. Koester, and J. H. Smith, Phys. Rev. 133, B117 (1964).
[6]J. R. Stewart, R. C. Morrison, and J. S. O'Connell, Phys. Rev. 138, B372 (1965).
[7]M. L. Halbert, P. Paul, K. A. Snover, and E. K. Warburton, in *Proceedings of the International Conference on Few Particle Problems in the Nuclear Interaction, Los Angeles, 1972,* edited by I. Slaus, S. A. Moszkowski, R. P. Haddock, and W. T. H. van Oers (North-Holland, Amsterdam, 1972).
[8]C. C. Chang, E. M. Diener, and E. Ventura, Phys. Rev. Lett. 29, 307 (1972).
[9]C. C. Chang, W. R. Dodge, and J. J. Murphy, II, Phys. Rev. 9, 1300 (1974).
[10]J. L. Matthews, T. Kruse, M. E. Williams, R. O. Owens, and W. Savin, Nucl. Phys. A223, 221 (1974).
[11]D. M. Skopik, J. J. Murphy, II, Y. M. Shin, K. F. Chong, and E. L. Tomusiak, Phys. Rev. C 11, 693 (1975).
[12]B. F. Gibson and D. R. Lehman, Phys. Rev. C 11, 29 (1975).
[13]I. M. Barbour and A. C. Phillips, Phys. Rev. C 1, 165 (1970).
[14]J. A. Hendry and A. C. Phillips, Nucl. Phys. A211, 533 (1973).
[15]I. M. Barbour and J. A. Hendry, Phys. Lett. 38B, 151 (1972).
[16]R. Nath, F. W. K. Firk, and H. L. Schultz, Nucl. Phys. A194, 49 (1972).
[17]H. F. Glavish, in *Proceedings of the International Conference on Photonuclear Reactions and Applications, Asilomar, 1973* (U.S. Atomic Energy Commission Office of Information Service, Oak Ridge, Tennessee, 1973), p. 755.
[18]H. R. Weller *et al.*, Phys. Rev. C 13, 922 (1976).
[19]T. B. Clegg, G. A. Bissinger, and T. A. Trainor, Nucl. Instrum. Methods 120, 445 (1974).
[20]S. Matsuki, M. Yasue, and S. Yamashita, Nucl. Instrum. Methods 94, 387 (1971).
[21]T. B. Clegg and W. Haeberli, Nucl. Phys. A95, 608 (1967).
[22]R. E. Marrs, E. G. Adelberger, K. A. Snover, and M. D. Cooper, Phys. Rev. Lett. 35, 202 (1975).
[23]Evans Hayward, William R. Dodge, and Bryan H. Patrick (unpublished).
[24]R. C. McBroom, Ph.D. thesis, University of Florida, Gainesville (unpublished).
[25]L. I. Schiff, Phys. Rev. 52, 242 (1937).
[26]*Neutron Cross Sections*, 2nd edition, edited by D. J. Hughes and J. A. Harvey (U.S.A.E.C., Washington, D. C., 1955).
[27]R. W. Carr and J. E. E. Baglin, Nucl. Data Tables 13, 500 (1974).
[28]R. M. Laszewski and R. J. Holt, At. Data Nucl. Data Tables, 19, 305 (1977). Note that these tables contain a phase error which was pointed out to us by R. G. Seyler, Physics Department, Ohio State University, Columbus, Ohio.
[29]B. D. Belt, C. R. Bingham, M. L. Halbert, and A. van der Woude, Phys. Rev. Lett. 24, 1120 (1970).
[30]B. F. Gibson and J. S. O'Connell, Phys. Lett. 32B, 331 (1970).
[31]E. L. Tomusiak, private communication.
[32]P. T. Kan *et al.*, Phys. Rev. C 12, 1118 (1975).
[33]B. D. Belt, thesis, University of Tennessee, 1970 (unpublished).
[34]J. H. Hubbell, Report No. NSRDS-NBS29, U. S. Govt. Printing Office, 1969 (unpublished) and references cited therein.
[35]B. A. Craver, Y. E. Kim, and A. Tubis, Nucl. Phys. A276, 237 (1977).
[36]W. Wölfli, R. Bösch, J. Lang, R. Muller, and P. Marmier, Helv. Phys. Acta 40, 946 (1967).
[37]O. Nathan and S. G. Nilsson, in *Alpha, Beta, and Gamma-Ray Spectroscopy*, edited by K. Siegbahn (North-Holland, Amsterdam, 1965), Chap. X.